Summer 2015

Identification of three novel genes, *PPK12*, *PPK23*, and *PPK25*, involved in noxious cold detection in *Drosophila*

Benjamin Williamson
James Madison University

Identification of Three Novel Genes, *ppk12*, *ppk23*, and *ppk25*, Involved in Noxious Cold Detection in *Drosophila*

Benjamin Williamson

A thesis submitted to the Graduate Faculty of

JAMES MADISON UNIVERSITY

In

Partial Fulfillment of the Requirements

for the degree of

Master of Science

Department of Biology

August 2015

Dedication Page

I dedicate this thesis to my grandfather Dr. Werner G. Deuser,
for sharing with me his passion for science and nature.

Acknowledgments

I would like to thank Dr. Timothy Bloss and Dr. Mark Gabriele for their help and expertise in RNA interference and neurophysiology and also for their support as members of my committee through the process of completing this thesis. I thank Dr. Kristopher Kubow and Dr. Bisi Velayudhan for their support with microscopy and optogenetics. I thank Dr. Corey Cleland for his help in optogenetics and my understanding of the action potential. I thank Mark Starnes and Joe Rudman for their support in constructing the camera stand and for fixing the thermal cyclers. I thank Dr. Christopher Rose for generously allowing me to use his equipment. I also would like to thank all of the undergraduates for their hard work in the lab including Haley Nisson, Harold Burke, Stephen Jurko, Jena Butler, Laura Johansen, Shannon Fox, and Ryan Samuel.

I would like to give an extra special thanks to Dr. Daniel N. Cox and Kevin Armengol whose work made this project possible. I thank Dr. Susan R. Halsell for her exceptional effort in guiding me through the process of writing this thesis and for giving me the chance to work with her which has truly changed my life forever.

Finally I thank the Biology Department of James Madison University and our funding through the 4VA grant to Halsell and Cox.

Table of Contents

List of Tables

List of Figures

ABSTRACT

The reflexive response and perception of pain (nociception) is an evolutionarily conserved process in animals. Pain can be a major health concern and current treatments often prove insufficient, especially in regards to chronic pain. Greater understanding of the molecular processes underlying pain sensation could lead to new and more effective treatments. The aim of this study is to investigate the molecular mechanisms of cold nociception in *Drosophila melanogaster.* A specific subset of peripheral sensory neurons (Class III dendritic arborization (da) neurons), are implicated in *Drosophila* larvae's response to noxious cold.

Previous literature has implicated a variety of ion channel families, including transient receptor potential (TRP) and degenerin/epithelial sodium channels (DEG/ENaC) family members, in mediating sensory responses to noxious heat and mechanosensation. Though much is known about noxious mechanical and heat nociception in *Drosophila*, little is known regarding the molecular components mediating cold nociception.

Here we focus on characterization of *Drosophila* DEG/ENaC family members as potential regulators of noxious cold-evoked sensory behavior. A novel behavioral assay, coupled with functional optogenetic studies and *in vivo* RNAi expression, has been utilized to investigate the role of select *pickpocket* (*ppk*) family members. Our analyses reveal that *ppk12, ppk23,* and *ppk25* are required for noxious cold detection in larvae. These studies provide novel mechanistic insight into the molecular underpinnings of cold-evoked behavioral responses and demonstrate a previously uncharacterized function for DEG/ENaC molecules in cold nociception.

BACKGROUND AND SIGNIFICANCE

Nocicepton, Pain, and Available Treatments

An organism's ability to sense and react to changes in its environment is fundamental to its survival (Khuong and Neely 2013). This becomes especially important in detecting noxious or potentially harmful stimuli. This process of sensing and interpreting noxious stimuli is termed nociception or pain (Sulowski *et al*. 2011, Im and Galko 2011). There are many types of noxious stimuli including mechanical, chemical and thermal (Im and Galko 2011).

Though pain is important for injury avoidance, it can also be detrimental to health and quality of life (Khuong and Neely 2013, Salat *et al*. 2013). Pain can be categorized as acute or chronic. Acute pain refers to perception of a current problem such as noxious stimuli or tissue damage (Salat *et al*. 2013). Though this process may be useful in injury avoidance, it can also decrease quality of life. Chronic pain, on the other hand, is viewed as unnecessary as it can occur without external stimuli or the presence of damaged tissue (Salat *et al*. 2013). It can develop through changes in the central nervous system (CNS) and is often characterized by a lowered pain threshold (allodynia), and increased sensitivity to certain stimuli (hyperalgesia) (Im and Galko 2011). Therefore, it is considered to be an illness and affects 30-60% of the global population, and upwards of 90% of the elderly population (Khuong and Neely 2013, Salat *et al*. 2013, Milinkeviciute *et al*. 2012).

Current treatments for pain are not effective for all types of pain, may not effectively control the pain, and/or may have unwanted side effects (Khuong and Neely 2013, Salat *et al*. 2013). Currently available treatments for pain often include exogenous opioids and non-steroidal anti-inflammatory drugs (NSAIDs) (Salat *et al*. 2013). Common examples of NSAIDs include aspirin and ibuprofen. NSAIDs inhibit cyclooxygenase (COX). COX is necessary for the conversion of arachidonic acid into prostaglandins. Some of these prostaglandins, particularly PCE2 and PCF2a, are involved in nociceptor sensitization (Slater *et al.* 2010). Exogenous opioids bind opioid receptors. Activation of opioid receptors is a metabotropic process, which leads to activation of a G-coupled protein. This protein inhibits adenyl cyclase, which is necessary for conversion of ATP to cAMP. cAMP is then necessary for activation of many protein kinases and transcription factors which are necessary for neuronal function. Another

consequence of the lack of cAMP is increased sodium potassium pump activity causing hyperpolarization. The end result is decreased neural activity (Slater *et al.* 2010).

Both NSAIDs and opioids have their own benefits and shortcomings. The anti-inflammatory drugs work well for low severity pain and can be localized to specific areas, but side effects include ulcers and kidney damage. Opioids are the most powerful of current pain medications, but have a huge array of problems including low specificity, constipation, difficulty breathing, tolerance, and of course addiction (Salat *et al*. 2013). Chronic pain in particular has been very difficult to treat largely due to a lack of understanding of its molecular mechanisms (Salat *et al*. 2013). Determining these mechanisms in greater detail will likely lead to improvements in the treatment of both acute and chronic pain.

Nociception: The *Drosophila* Model System

Nociception is an evolutionarily conserved process and many of the genes involved have conserved function across species as diverse as humans and insects (Im and Galko 2011, Milinkeviciute *et al*. 2012). Ion channels in particular are highly conserved in the metazoans. Ion channel proteins are critical for sensory function and many are involved in nociception (Adams *et al.* 1998, Tracey *et al.* 2003, Zhong *et al.* 2009, Kim *et al.* 2010, Aldrich *et al.* 2010, Im and Galko 2011, Sulowski *et al*. 2011). Studies on ion channel genes have been conducted in model systems including *C. elegans,* mice, zebra fish, and *Drosophila*.

RNA interference techniques are an effective means for studying protein function. Though this technique is highly utilized in both *C. elegans* and *Drosophila*, the ability to specify the tissue where RNAi will be expressed is much easier in *Drosophila*. This advantage (discussed below) is a major reason the metazoan *Drosophila melanogaster* is a good model organism for the study of the molecular mechanisms of nociception in peripheral sensory neurons (Milinkeviciute *et al*. 2012).

Peripheral sensory neurons responsible for reflexive pain sensation are termed nociceptors (Loeser and Treede 2008). These neurons are characterized by naked dendrites that interdigitate with epithelial cells (Grueber *et al*. 2002). When triggered in vertebrates, these nociceptors simultaneously send signals to the central nervous system along two paths (Fig. 1). The first path sends the message to the central nervous system where it arcs back to the motor neurons causing a reflex reaction termed the nocifensive response.

At the same time the message is also delivered on a second path to the brain for processing as a pain sensation.

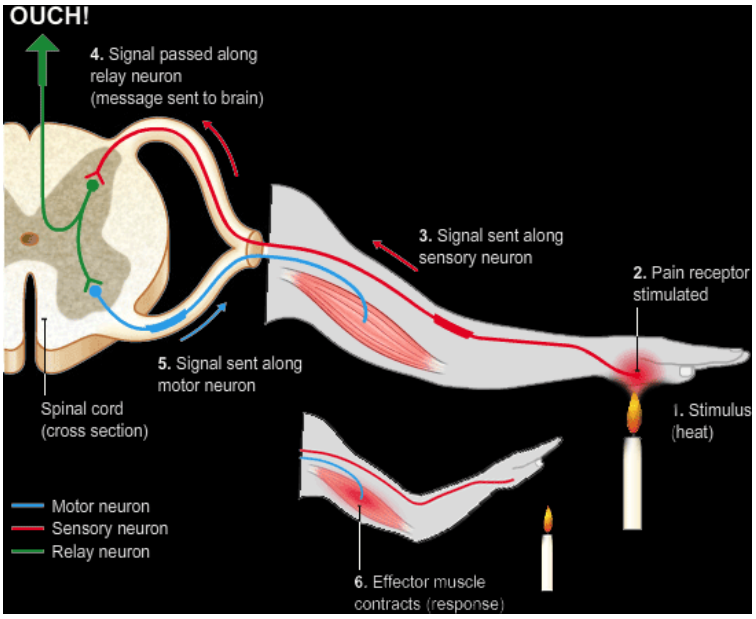

Figure 1. Nocifensive response and reflex arc. When a nociceptor senses a noxious stimulus such as heat, cold, chemical, or mechanical, the signal is first transduced into an action potential which is then passed along the nociceptor (red) to nerves in the spinal cord (green). At this point, the signal is transduced exciting a motor neuron (blue) to evoke the muscular nocifensive response (or reflex movement). At the same time as the signal is passed to the motor neuron by the relay neuron, it is also passed to the brain where the signal is interpreted as pain. None of the neurons depicted directly interact with the white matter of the CNS, but rather penetrate through it. Source: https://www.xtremepapers.com/revision/gcse/biology/co-ordination_and_response.php

The *Drosophila* peripheral nervous system (PNS) is composed of both single and multidendritic sensory organs designated type I and II. Type I includes external sensory organs [es] and chordotonal sensory organs [ch] and are single dendritic. Type II neurons are called multidendritic neurons [md]. Mds are subdivided into dendritic arborization [da], tracheal dendrite [td], and bipolar dendrite [bd] neurons (Iyer *et al*. 2013). da neurons are of particular interest. The da neurons are categorized as classes I, II, III, or IV in order of increasing branching complexity (Fig. 2; Im and Galko 2011). The da neurons have naked dendritic projections that extend out to the epidermis; they are architecturally and functionally similar to the free nerve endings found in vertebrate nociceptors (Milinkeviciute *et al*. 2012).

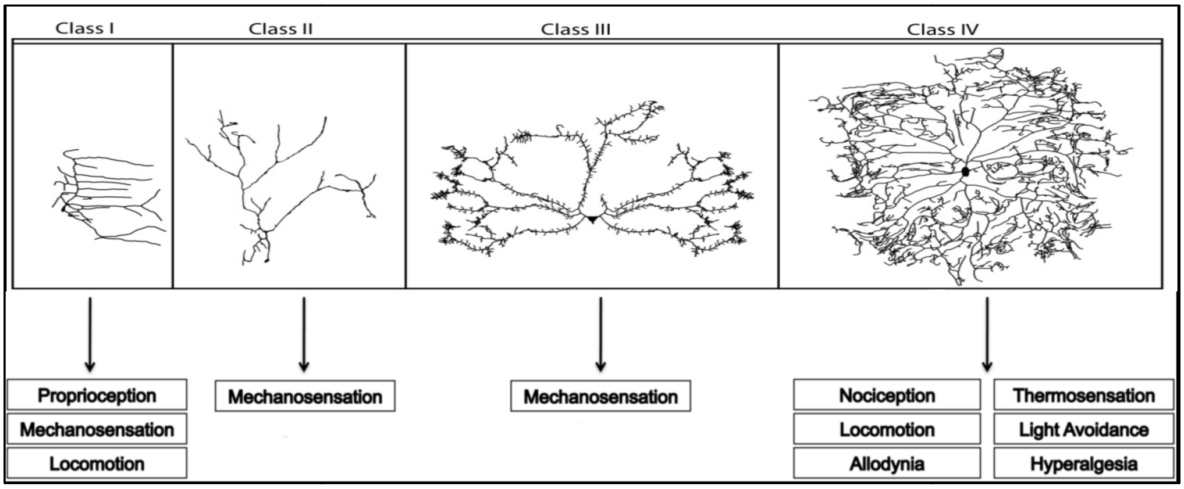

Figure 2. Four classes of *Drosophila* larval da neurons and currently known sensory functions. Recently Class III da neurons have been implicated in cold nociception (Dan Cox personal communications). Figure from: Sullivan, *et al.* (2013).

The different classes of da neurons participate in different sensory functions (Fig. 2). Some of these sensory functions are shared between multiple classes while others are restricted to a single class type. For example noxious heat is known to be almost exclusively interpreted by class IV, while mechanical sensation is divided between classes I, II, III and IV (Im and Galko 2011). The molecular mechanisms of many of these sensory functions have been well characterized. However, little is known about the molecular basis of chemical and cold nociception (Sullivan *et al*. 2013). This project particularly focuses on the molecular mechanisms of cold nociception. The choice to study pain using the cold stimulus has one major advantage above other stimuli. Work done by Dr. Daniel Cox's labs at George Mason University and now at Georgia State University has shown that the cold stimulus is sensed primarily by the Class III (CIII) da neurons (Dan Cox personal communications). Larvae expressing tetanus toxin in CIII da neurons had a diminished reflex to noxious cold, optogenetic stimulation of CIII da neurons mimicked the reflex response to noxious cold, and GCaMP studies on larvae exposed to noxious cold showed activation of primarily CIII da neurons. This simplifies the analysis because we can focus on a single class of da neurons.

The da neurons have been extensively characterized in *Drosophila* third instar larvae. This stage is important because earlier larval stages do not have fully developed neural circuits particularly at the neuromuscular junctions (NMJ), which impedes the nocifensive response (Sulkowski, *et al.* 2011). The behavioral response to noxious cold has been characterized for the third instar larvae by Daniel Cox's lab

and a simple behavioral assay has been developed and is discussed below. It is also important to use larvae because the adults have a thick cuticle that is not penetrable by light whereas the larval epidermis is transparent. This is important for optogenetic experiments that require light to penetrate to the neurons (discussed in Methodology).

Drosophila Cold Nociception: Candidate Ion Channels

Two families of ion channel subunit encoding genes have been implicated in *Drosophila* nociception through experiments with mechanical and heat stimuli; these include the degenerin epithelial sodium channel (DEG/ENaC) family and the transient receptor potential (TRP) ion channel family (Cox personal communication, Montel 2005, Rosenweig *et al.* 2008, Driscoll 2010, Zhong *et al*. 2010, Zelle *et al.* 2013, Bianchi and Salat *et al.* 2013).

The DEG/ENaC family is composed of 31 known members in *Drosophila* in contrast to 9 in mammals (Zelle *et al.* 2013). These genes have been named the *pickpocket* (ppk) genes. The general structure of their encoded proteins includes two membrane spanning regions and a cysteine rich domain on the extracellular side of the membrane, which is involved in receptor function (Fig. 3; Bianchi and Driscoll 2010). As their name suggests these proteins form ionotropic channels that generate Na^+ currents (Zelle *et al.* 2013). All are inhibited by the diuretic amiloride, a readily available drug with a short half-life, which is known to have antinociceptive effects (Jeong *et al.* 2013). These genes are fairly diverse in function with respect to their ligands and their response to various stimuli.

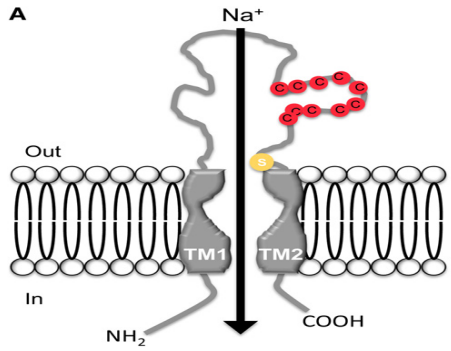

Figure 3. General structure of degenerin epithelial sodium channel subunit. The structure contains 2 transmembrane regions and an extracellular cysteine rich receptor binding loop (shown in red). Figure from Zelle *et al.* 2013.

DEG/ENaC family members encode ion channel subunits, which are thought to combine to produce trimers, which constitute functional sodium channels. Some members can form homotrimers on their own such as *ppk2*, while others form heterotrimers such as the combinations *ppk23/ppk29, ppk11/ppk16, ppk11/ppk19* and *ppk/ppk26* (Adams *et al.* 1998, Gautam *et al.* 2002, Zelle *et al.* 2013, Gorczyca *et al.* 2014). It is also thought that the gene products of *ppk25, ppk23* and *ppk29* form a heterotrimer. This suggests that these trimers can be composed of one, two, or three different subunits.

The individual members of this group are not well characterized and many of their specific physiological roles remain unknown (Adams *et al.* 1998, Bianchi and Driscoll 2010). However, it is known that *ppk4* and *ppk11* are involved in liquid clearance in the *Drosophila* trachea, the combination of *ppk/ppk26* contributes to mechanical nociception, and *ppk25, ppk23* and *ppk29* are involved in pheromone detection (Liu *et al.* 2003, Lu *et al.* 2012, Vijayan *et al.* 2012, Gorczyca *et al.* 2014).

Even less is known about the specific neurological function of the DEG/ENaC's with regards to transduction or propagation of stimuli. Transduction refers to the primary detection of the stimulus which is transduced into an action potential (Fig. 4). Propagation refers to the process of the movement of the action potential from the peripheral dendrites along the axon and toward the central synapse connecting the sensory neuron to the spinal cord. The mouse DEG/ENaC channel subunits ASIC1a, ASIC2, and ASIC3 are involved in the propagation phase of mechanical sensation, while the subunit encoded by *ppk* is thought to be involved in mechanotransduction (Zhong 2011, Raouf *et al.* 2012). This suggests that the DEG/ENaC subunits are capable of both transduction and propagation.

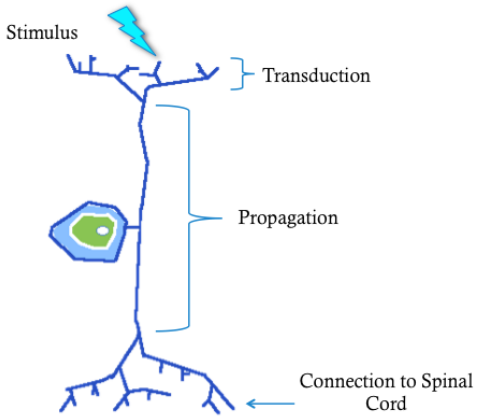

Figure 4. Difference between transduction and propagation of a stimulus. The stimulus (indicated by the blue lightning bolt activates the ion channels responsible for transduction which then initiate an action potential. Another group of ion channels propagate the signal across the neuron where it can be transmitted to the central nervous system

The TRP ion channel family has been studied in other types of nociception, particularly in detection of noxious mechanical and thermal stimuli. The human TRPM8 gene is known to function in cold nociception (Feketa *et al.* 1997). There are 13 known *Drosophila* TRP genes compared to 27 human genes. Despite fewer known genes, *Drosophila* contain at least one gene in all seven of the TRP subfamilies (Jegla *et al.* 2009). The TRP subunit structure consists of six transmembrane regions (Fig. 5). These are calcium channels that exhibit both voltage and ligand gated characteristics, and therefore do not fit nicely into either channel classification (Minke 2010). Interestingly, menthol is a known ligand for the TRPM8 channel, which when bound gives the perception of cold. The name transient receptor potential originates from the *Drosophila* mutant of this gene, which displayed a transient response to light (Cosens 1969). These channels function in numerous processes including mechanical, thermal and cold nociception, osmoregularity, light perception and more (Montel 2005, Rosenweig *et al.* 2008, Salat *et al.* 2013). Previous studies using behavioral assays in *Drosophila* larvae have identified TRP genes function during nociception. Two examples include *painless* which has been implicated in thermal and mechanical nociception (Tracey *et al.* 2003) and *piezo*, which contributes to mechanical nociception (Kim *et al.* 2010). The involvement of these proteins in nociception increases the likelihood that some may play a role in cold nociception.

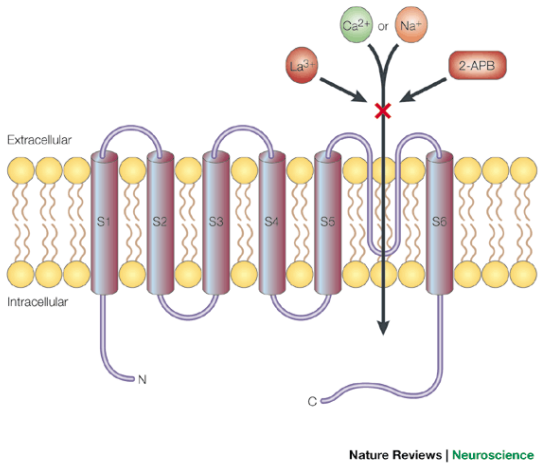

Figure 5. General structure of a transient receptor potential ion channel protein. The channel includes 6 transmembrane regions and can be activated by either voltage or ligand binding. Figure from Clapham *et al.* 2010.

Drosophila Cold Nociception: Selecting Specific Gene Targets for Study

Microarray studies performed in Dr. Cox's lab have shown differentially expressed genes in the CIII da neurons compared with CI, CII, and CIV (personal communication). The noteworthy results included members of the DEG/ENaC family and the TRP family. Since CIII's are the primary cold nociceptors, it is likely that members of these two gene families are involved in cold nociception, as expected due to their function in mechanical and heat induced nociception. The CIII enriched TRP genes include the following with fold enrichment indicated in parentheses: *trp* (2.2x), *trpγ* (6x), *painless* (11.2x), *trpm* (24x), *trpml* (9.5x), *nompc* (8.6x), and *Pkd2* (63x). In addition to these TRP genes three genes from the *pickpocket* family of DEG/ENaC's were also enriched including *ppk12* (10.1x) , *ppk23* (10.4x), and *ppk25* (28.5x).

Some of these genes already have known nociceptive function. As mentioned earlier, *painless* is involved in thermal and mechanical nociception (Tracey *et al.* 2003). *nompc* is involved in mechanosensory transduction, and inhibition of the behavioral response to cold (Dan Cox, personal communication). It is not surprising that the *trpm* encoded channels were enriched, as TRMP8 is involved in mammalian cold detection (Feketa *et al.* 1997). Since less is known about the roles of DEG/ENaC members, this research focused on the three *pickpocket* genes, *ppk12, ppk23,* and *ppk25*. Currently little is

known about these three genes with respect to nociception. However *ppk23* and *ppk25* are known to detect pheromones and are essential for courtship (Pikielny et al. 2012, Vijayan *et al*. 2014).

Statement of Hypothesis

At least one of these three members of the DEG/ENaC *pickpocket* family (*ppk12, ppk23,* and *ppk25*) function in Class III da neuronal mediation of larval nociceptive cold behavioral response. Further, each may function in either the transduction of cold sensing or subsequent central propagation within the Class III da neurons.

METHODOLGY AND EXPERIMENTAL APPROACH

Summary of Experimental Approach

This project seeks to determine the possible roles of *ppk12, ppk23,* and *ppk25* in cold nociception in *Drosophila melanogaster*. Previous work has shown that CIII da neurons are primarily responsible for the cold response. Furthermore two ion channel groups (TRP and DEG/ENaC) are differentially expressed in the CIII da neurons (Dan Cox, personal communication). Cold plate behavioral assays were performed with third instar larvae expressing RNAi for *ppk12, ppk23* or *ppk25* in Class III (CIII) da neurons or with loss-of function alleles for each of these genes (Fig. 6). If a functional role for one of these DEG/ENaC family members was suggested, by the behavioral assay, then the gene was tested again in an optogenetic assay to determine function in transduction or propagation of the stimulus (Fig. 4).

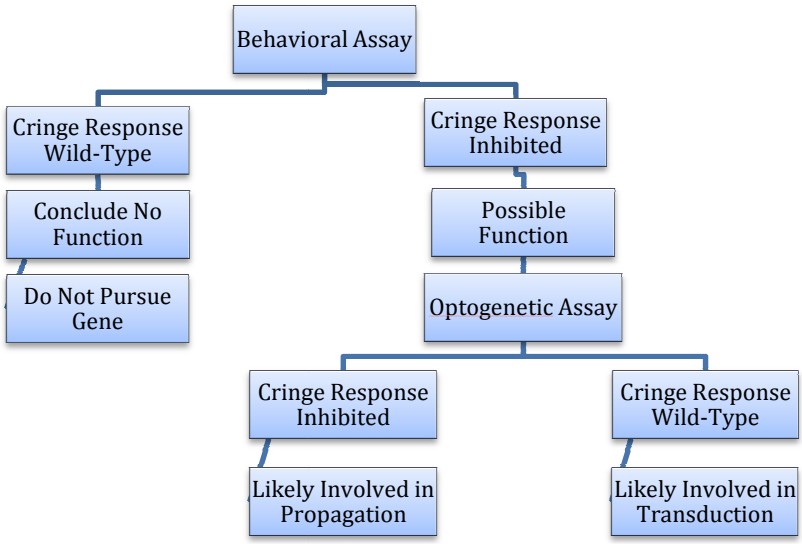

Figure 6. Methodology flow chart for determining possible *ppk* channel function in *Drosophila* cold nociception. Change in behavior from wild-type in the behavioral assay will warrant further study with the optogenetic assay to determine function in transduction or propagation.

Class III da Neuron Specific Knockdown of *ppk* Gene Expression

The Gal4/UAS Expression System

In order to reduce the expression of the *ppk* genes in CIII da neurons, the Gal4/UAS system was used to drive cell specific RNAi expression. The Gal4 protein and upstream activating sequence (UAS) function in control of transcription in yeast (Duffy 2002). This system has been employed in many

organisms but most frequently in *Drosophila.* The Gal4 gene (also known as the driver) encodes a transcription activator protein that specifically binds to the upstream activating sequence (UAS), analogous to an enhancer element of the responder gene. When bound to the UAS, Gal4 drives transcription of the responder gene which is expressed under the control of the UAS (Fig. 7, upper panel). The Gal4 gene is controlled by a promoter containing enhancer like elements specific to the *Drosophila* cells being studied (Fig. 7, upper panel). In this study, Gal4 expression was driven by a CIII da neuron specific promoter (Gal4 line 19-12; Tables 2 and 3; Xiang *et al*. 2010). When a CIII da Gal4 driver line is crossed to a UAS line bearing a *ppk* RNAi construct, (Table 1) the progeny containing both transgenes will express the RNAi exclusively in their CIII da neurons.

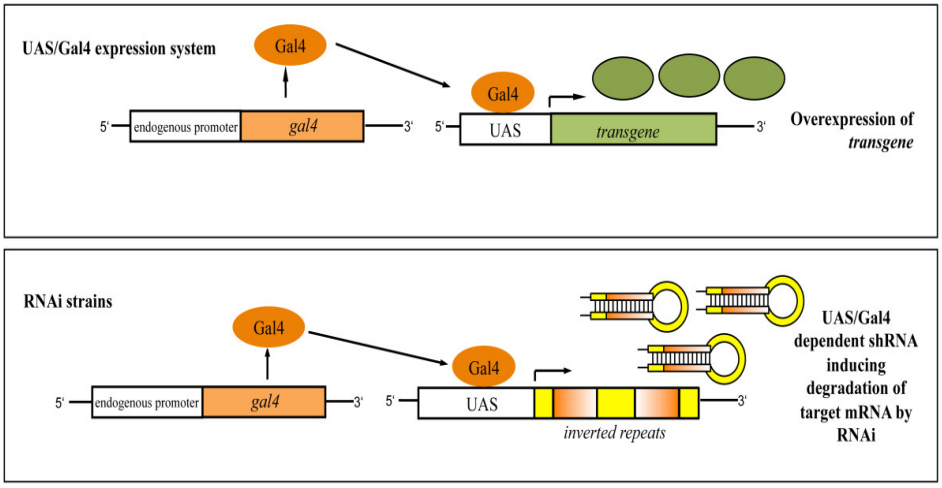

Figure 7. Gal4/UAS method of RNA interference in *Drosophila*. The top panel shows Gal4 transcription activator protein binding the UAS to express a responder transgene. The bottom panel shows this process used to express an inverted repeat which then transforms into a small hairpin RNA (shRNA) for RNA interference. Modified from Prubing *et al.* 2013.

RNA Interference (RNAi) Induced Knockdown of Gene Expression

Each of the UAS RNAi transgenes used in this study encode an inverted repeat of one of the three *ppk* genes. When transcribed, this inverted repeat folds over on itself to form a small hairpin RNA (shRNA) (Fig. 7, lower panel; Prubing *et al.* 2013, Singh and Ganguli, 2013). The shRNA induces the RNA interference pathway whereby the Dicer-2 protein cuts it into small inhibiting RNAs (siRNA) that are then bound by a number of proteins into the RNA induced silencing complex (RISC). Subsequently this complex binds to the cognate mRNAs. This either induces the degradation of the cognate mRNA or the

inhibition of its translation. As a consequence, the expression of the gene of interest, in this case, *ppk12, ppk23*, or *ppk 25,* is reduced (knocked down).

Generation of Stable Transgenic Lines in Drosophila

Drosophila mutant lines are created through a process of transgenic insertion. This process starts with a P-element, a DNA transposon specific to *Drosophila* (Bachman and Knust, 2008). The P-element transposon consists of a gene encoding a transposase flanked by P-element inverted repeats. For generation of genome incorporated transgenes, the P-element is modified by standard molecular techniques. Modifications include insertion of a marker gene, such as the *white* eye color gene, that gives rise to an easily distinguishable phenotype in transformed animals. The experimental gene or RNAi construct of interest is also inserted between the P-element ends. The P-element transgene construct is injected into the posterior end of *Drosophila* syncytial blastoderm embryos. Some of this DNA will be stably incorporated into the genome of a germline cells. Transposition of the transgene construct is random. Transformed flies are selected by crossing of the resulting adults and identification of their progeny that express the phenotypic marker.

Most *Drosophila* UAS RNAi lines are created using the *Drosophila* P-element system. The P-element inserts randomly in the genome. A consequence of the random insertion is that the expression level can vary significantly depending on where the transgene inserted in the genome. Each new *Drosophila* line must therefore be optimized to create a sufficiently strong phenotype. Adding more copies of the gene and strong promoter sequences can increase the level of expression (Jian-Quan *et al.* 2007). Strength of the phenotype can then be determined visually or by other more quantitative methods such as fluorescence intensity or loss of function assays depending on what works best for the particular target gene (Jian-Quan *et al.* 2007). Conformation of RNAi as the source of the phenotypic change can be determined via PCR and western blotting.

Assays of *Drosophila* Larval Responses to Noxious Cold

Cold Plate Behavioral Assay

The behavioral response of the wild-type *Drosophila* third instar larvae to noxious cold has been characterized by Daniel Cox's lab and replicated in the Halsell lab (Dan Cox, personal communication).

The habitable temperature range for *Drosophila* is 19-29°C. At these temperatures in the behavioral assay the larvae crawl freely. At approximately 12°C the larvae begin to raise their heads and tails and decrease their crawling movement. At 10°C they begin to exhibit an anterior-posterior contraction, termed "cringing" (Fig. 8). This cringe behavior is maximized and crawling minimized at ≤ 6°C. RNAi *ppk 12, ppk23,* and *ppk25* transgenes and also loss-of-function mutants for *ppk12* and *ppk 23* were tested (see Methods).

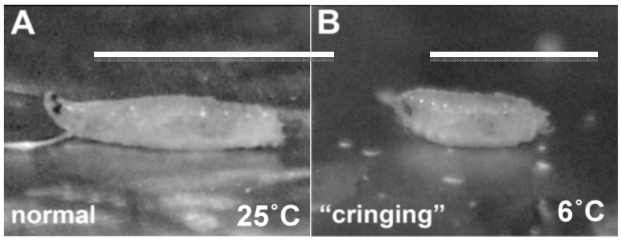

Figure 8. Nocifensive response of the *Drosophila* third instar larvae to noxious cold. This behavior is an anterior-posterior contraction termed "cringing" and is maximized at ≤ 6°C. Note the overall length of the larva at 25°C is longer than at 6°C (white bars). Modified from: Sullivan, *et al.* (2013).

The behavioral assay was used to determine if knocking down *ppk 12, ppk23,* or *ppk25* expression would cause an inhibition of the cringe response to noxious cold. If knockdowns of any of these genes inhibits the response, then it is concluded that the gene products are necessary for noxious cold detection.

Optogenetic Assay

If one of the *ppk* channel proteins is identified by the behavioral cold plate assay as required for cold nociception, then the question is whether the channel protein is required in the transduction of the noxious cold stimulus and/or the propagation of the stimulatory action potential. An optogenetic assay allows us to differentiate between these two possibilities. Optogenetics allows for activation of neurons with light. It works by utilizing a light-gated ion channel found in photoreceptors of the green algae *Chlamydomonas reinhardtii* (Fig. 9, Husson *et al.* 2013). For this project an engineered version of channelrhodopsin-2 (ChR-2) with an amino acid switch from threonine (T) or alanine (A) to glutamic acid (E) at amino acid position 123 was used. This modified ChR2 is termed ChETA. This amino acid modification results in channel proteins that activate in the millisecond timeframe (Honjo *et al.* 2012). Speed is important because delay in response could lead to a false negative result (discussed below). The ChETA protein can only function in the presence of a chromophore molecule called all-trans retinal (ATR).

The ATR molecule works as a cofactor for the ChETA channel by absorbing a photon of light allowing for conversion from an all trans state to a 13-cis state (Fig. 10). This change in shape of the chromophore cofactor ATR causes conformational change in the ChETA ion channel to allow the passage of ions (Fig. 9). The ATR molecule quickly goes back to the trans conformation in the dark causing the closing of the ion channel (Umezaki *et al.* 2011; Caro *et al.* 2012). Stimulation by blue light of this heterologous ion channel circumvents the transduction requirement in the neuron in which it is expressed.

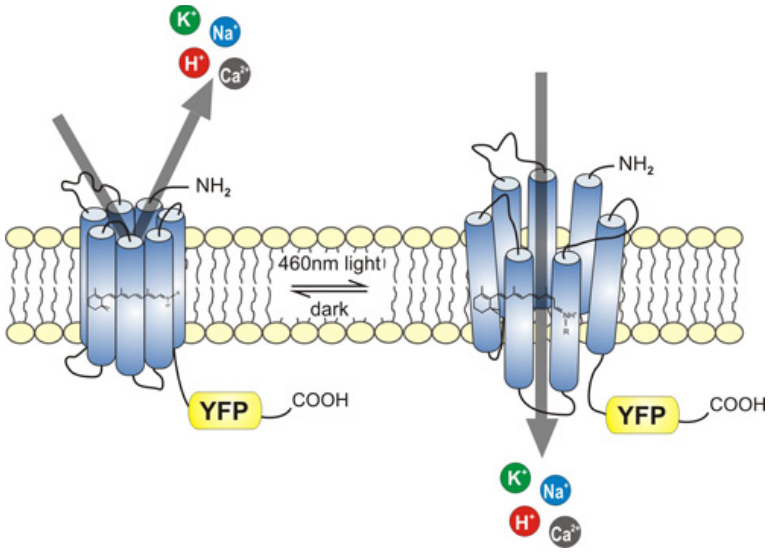

Figure 9. Channel rhodopsin 2 channel activation by blue light. When 480nm blue light hits the all-trans retinal chromophore, it converts to a 13-cis conformation, which opens the channel. YFP refers to yellow fluorescent protein and is used as a visual marker of channel expression. Source: Bamberg 2014

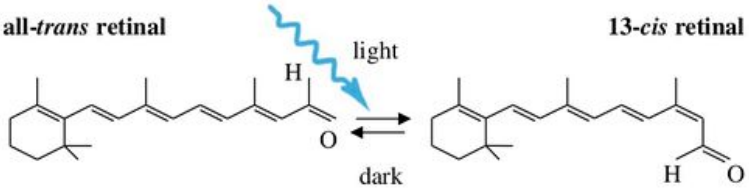

Figure 10. Conformational change of all-trans to 13-cis retinal in presence of 480nm blue light. Source: Wong *et al.* 2012.

.

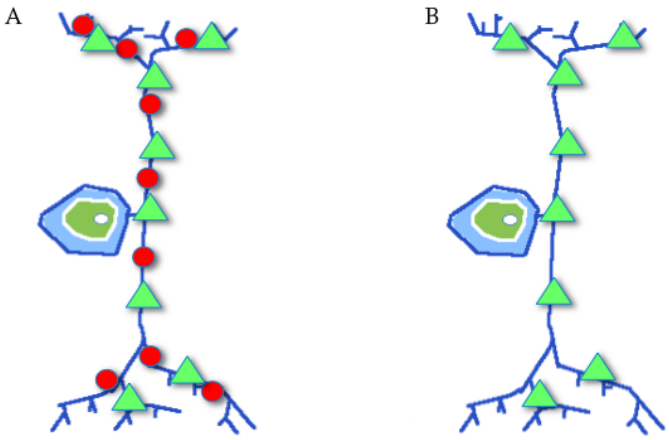

Figure 11. Conceptualization of the *ppk* optogenetic assay. Both A and B represent Class III da neurons. Panel A represents the ChETA channel expressed (green triangles) along with the normally expressed *ppk* channel of interest (red circle). Panel B represents the expression of the ChETA channel and knockdown of the *ppk* channel with RNAi. Activation of the ChETA channels with blue light replaces the noxious cold induced transduction phase. If the lack of the *ppk* channel inhibits the blue light triggered cringe response, then the *ppk* channel is likely to be involved in propagation.

The optogenetic assay induces the cold nociceptive behavioral response at room temperature in response to blue light stimulation (this study, see below; Dan Cox personal communication). Figure 11 shows the process of combining expression of the light gated ChETA channel with RNAi to determine if a *ppk* subunit is involved in transduction or propagation. By knocking down the *ppk* subunit and stimulating the neuron with blue light, any inhibition of the cringe response should be due to a break in the propagation phase while a full cringe response suggests the *ppk* functions in the transduction phase. (Honjo *et al.* 2012). Procedurally, the analysis of the optogenetic assays is very similar to the cold plate behavioral assay analysis. In this case the Gal4/UAS system is used, ßnot only to express the RNAi *ppk* constructs in CIII da neurons, but also to simultaneously drive expression of the blue light activated ChETA ion channel. The experimental optogenetic assay larvae are fed ATR and larvae of the same genotype not fed ATR serve as the negative control.

METHODS

Drosophila Stocks and Crosses

Gal4 driver lines were maintained as separate stocks from the UAS responder lines (Table 1). The lines were then crossed to produce the desired genotype (Tables 2 and 3). Third instar larvae were selected for analysis. To control for possible false positive/negative results, when possible, multiple independent UAS RNAi constructs were tested as well as mutant lines for channel genes of interest.

Oregon R was used as the wild type line. The CIII GAL4 driver for the cold assay was 19-12 tdGFP which expresses the GAL4 protein in the CIII neurons (Xiang *et al.* 2010) . The CIII GAL4 driver for the optogenetic assay was 19-12 ChETA which expresses both the GAL4 protein and the ChETA subunit which forms blue light gated channels in the CIII neurons. The UAS responders include a total of five UAS RNAi constructs including UAS *ppk12A,* UAS *ppk23,* UAS *ppk25A,* UAS *ppk25B,* and UAS *ppk25C,* and the positive experimental control UAS TNTE. The UAS TNTE responder encodes the tetanus toxin light chain (Sweeny *et al.* 1995).. When expressed, this protein cleaves synaptobrevin, which is a protein necessary for neurotransmitter exocytosis. This prevents synapses from occurring, which in our case means expression of TNTE in the CIII da neurons will stop them from passing their signal to the central nervous system and therefore inhibiting the reflex cringe response Therefore, UAS TNTE will be a positive control for inhibition of the cringe response. Three loss of function mutant lines included *ppk12* mutant, *ppk23* mutant A, and *ppk23* mutant B. The exact genotypes and stock numbers can all be found in Table 1.

Many control crosses were used in the assays (Tables 2 and 3). For the cold behavioral assay, the UAS responders were crossed to Oregon R as a negative control because without Gal4, UAS will not be activated. For the optogenetic assay the GAL4 drivers crossed to the UAS responders were grown with and without ATR.

Table 1. Stocks

Function	Stock Number	Genotype	Description	Alternative name
Wild Type	N/A[1]	Oregon R	Wild Type	OR
GAL4 CIII drivers	N/A[1]	19-12 tdGFP	CIII specific driver/ imaging	19-12 tdGFP
	N/A[1]	19-12.CHETA.YFP	ChETA CIII da Driver	19-12 ChETA
Control Responder	N/A[1]	UAS-TNTE	Tetanus Toxin	UAS TNTE
RNAi Responders	KK105131-VDRC[2]	UAS-*ppk12*[RNAi]	*ppk12* RNAi	UAS *ppk12*ARNAi
	N/A[1]	*y[1] v[1];* p[TRiP-JF02027] attP2	*ppk12* RNAi	UAS ppk12B RNAi
	KK106873-VDRC[2]	UAS-*ppk23*[RNAi]	*ppk23* RNAi	UAS *ppk23* RNAi
	KK10808-VDRC[2]	UAS-*ppk25*[RNAi]	*ppk25* RNAi	UAS *ppk25A* RNAi
	B-27086[3]	*y[1] v[1];* UAS-*ppk25*[RNAi]	*ppk25* RNAi	UAS *ppk25B* RNAi
	GD7343-VDRC[2]	UAS-*ppk25*[RNAi]	*ppk25* RNAi	UAS *ppk25C* RNAi
Loss of Function Mutants	B-29179[3]	*w; Mi{ET1}ppk12*^{MB11059}	*ppk12* mutant	*ppk12*
	B-12571[3]	*w; ppk23*^{BG01654}	*ppk23* mutant	*ppk23* allele A
	B-3330[3]	*w; ppk23*^{G17320}	*ppk23* mutant	*ppk23* allele B

Source of stocks:
1=Dan Cox, Georgia State University
2=Vienna Drosophila Resource Center
3=Bloomington Drosophila Stock Center

Cold plate Behavioral Assay

Wild type Oregon R were used as the first set of control larvae for the cold behavioral assay. This was considered a negative control because there should be no inhibition in the cringe response. Oregon R virgin females were also crossed to male UAS RNAi or UAS TNTE strains which served as another negative control due to lack of GAL4 protein binding UAS for expression of the RNAi or TNTE sequence. The experimental larvae were generated by crossing virgin females of the CIII da neuron GAL4 driver 19-12 tdGFP to male UAS RNAi or UAS TNTE strains which led to binding of GAL4 to the UAS and hence expression of the RNAi or TNTE sequence (Table 2). As mentioned above, UAS TNTE is a positive control to reveal cringe inhibition, however, procedurally it was treated similar to the UAS RNAi constructs in that it was crossed to both the GAL4 driver 19-12 tdGFP and to Oregon R.

To generate the appropriate larval genotypes, 20-25 virgin females were crossed with 10-15 males. Crosses were performed in 6 oz bottles containing 50mL of standard cornmeal/molasses food. All bottles were incubated at 25°C for 7-9 days. Third instar larvae were identified as those that were actively crawling up near the top of the bottle and were visually much larger than the first and second instar larvae, which stayed near the bottom in the food.

Table 2. Crosses, Genotypes, and Function of Larvae for Cold Plate Behavioral Assays

♀	♂	**Function in Assay**
OR	OR	Wild Type
OR	UAS TNTE	Tetanus Toxin control
19-12 TDGFP	UAS TNTE	Tetanus Toxin
OR	UAS *ppk12*	control
19-12 TDGFP	UAS *ppk12*	knockdown
OR	UAS *ppk23*	control
19-12 TDGFP	UAS *ppk23*	knockdown
OR	UAS *ppk25A*	control
19-12 TDGFP	UAS *ppk25A*	knockdown
OR	UAS *ppk25B*	control
19-12 TDGFP	UAS *ppk25B*	knockdown
OR	UAS *ppk25C*	control
19-12 TDGFP	UAS *ppk25C*	knockdown
UAS *ppk12* mutant	UAS *ppk12* mutant	loss of function
UAS *ppk23* mutant A	UAS *ppk23* mutant A	loss of function
UAS *ppk23* mutant B	UAS *ppk23* mutant B	loss of function

The cold-plate behavioral assay setup included a thermal cycler, a fiber optic light source, a Nikon 5200 camera mounted above the sample block of the thermal cycler, and a black painted aluminum plate (Fig. 12). The fiber optic lighting pointed horizontally across the sample block coupled with the black color of the aluminum plate enhanced the contrast of the white larvae against a black background. The sample block of the thermal cycler was flooded with water to ensure maximal temperature transfer. Next the

thermal cycler was powered up and set to remain at constant 5°C and allowed time to reach this temperature. 5°C was the temperature used in behavioral screening because in order to get the aluminum plate which rests on the sample block to get to ≤ 6°C the sample block needs to be 5°C. Approximately 120 third instar larvae were collected from the top of the bottle and rinsed with water before placing on a damp kimwipe. Larvae were left to crawl around the kimwipe.

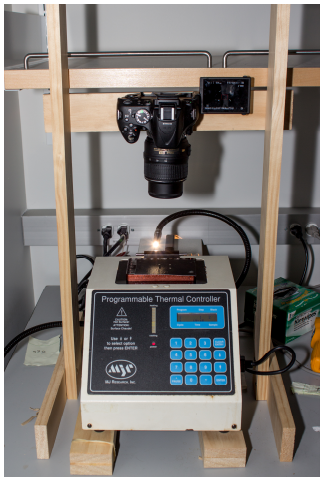

Figure 12. Cold Plate Behavioral Assay Setup. A Nikon 5200 is mounted directly above the sample block of a PTC-100 thermal cycler. Larvae are placed on an aluminum plate atop flooded sample block. Fiber optic lighting is used to direct light horizontally thereby fully illuminating the larvae without much illuminating of the black background plate.

To begin the assay, a standard spray bottle was used to spray a mist of water into the air. The black aluminum plate was then swept through the mist to collect a very fine mist of water droplets that covered the plate. Four actively mobile larvae were then taken from the damp kimwipe and placed in a small (~1.5cm) square in the middle of the misted black plate. Video recording was started at this time and the aluminum plate was subsequently pressed firmly against the flooded sample block. Video was recorded at 60 frames/sec for 30 seconds. This procedure was repeated for approximately 30 videos (approximately 120 larvae). Videos were analyzed as described below.

Optogenetic Assays

As mentioned above, the cringe response to cold can be mimicked at room temperature via blue light activation by expression of the ChETA blue light gated channel in the CIII da neurons of the third instar *Drosophila* larvae in the presence of ATR. The GAL4 driver 19-12 ChETA was used alone as the

first set of control larvae for the optogenetic assay. In addition to its role as a GAL4 driver, it also drives expression the ChETA blue light gated channel throughout the Class III da neurons. This was considered a negative control because there should be no inhibition in the blue light activated cringe response. The experimental larvae were performed by crossing virgin females of the CIII da neuron GAL4 driver 19-12 ChETA to male UAS RNAi or UAS TNTE strains which led to binding of GAL4 to the UAS and hence expression of the RNAi or TNTE sequence along with the ChETA light gated channel. All negative control and experimental larvae were grown in the presence of ATR while positive controls were grown without ATR. Just as in the cold behavioral assay, UAS TNTE is a positive control, however, procedurally it was treated similar to the UAS RNAi constructs in that crosses were performed on food with and without ATR.

Experimental and control larvae were generated by crossing10-15 virgin females with 5-10 males (Table 3). Larvae were grown in vials with 7 ml of food. Positive controls were grown on food with a final concentration of 0.1 mM ATR (Sigma). All vials were incubated at 25°C for 7-9 days.

Table 3. Crosses, Genotypes, and Function of Larvae for Optogenetic Assays

♀	♂	**ATR Added**	**Function in Assay**
19-12 ChETA	19-12 ChETA	no	Negative Control
19-12 ChETA	19-12 ChETA	yes	Positive Control
19-12 ChETA	UAS TNTE	no	Tetanus Toxin control
19-12 ChETA	UAS TNTE	yes	Tetanus Toxin
19-12 ChETA	UAS *ppk12A* RNAi	no	control
19-12 ChETA	UAS *ppk12A* RNAi	yes	knockdown
19-12 ChETA	UAS *ppk12B* RNAi	no	control
19-12 ChETA	UAS *ppk12B* RNAi	yes	knockdown
19-12 ChETA	UAS *ppk23* RNAi	no	control
19-12 ChETA	UAS *ppk23* RNAi	yes	knockdown
19-12 ChETA	UAS *ppk25A* RNAi	no	control
19-12 ChETA	UAS *ppk25A* RNAi	yes	knockdown
19-12 ChETA	UAS *ppk25B* RNAi	no	control
19-12 ChETA	UAS *ppk25B* RNAi	yes	knockdown
19-12 ChETA	UAS *ppk25C* RNAi	no	control
19-12 ChETA	UAS *ppk25C* RNAi	yes	knockdown

The optogenetic assay setup was similar to the cold behavioral assay setup but includes a Leica fluorescent scope in the place of the thermal cycler and fiber optic light source. A Nikon 5200 camera was mounted to the observation tube of the fluorescent scope. A glass plate was used in place of the black aluminum plate and was placed on the microscope stage. A small amount of back light was used to illuminate the larvae through the glass compared to a dark background. The fluorescent filter was set to GFP. Approximately 120 third instar larvae were collected from the top of the bottle and rinsed with water before placing on a damp kimwipe. Larvae were left to crawl around the kimwipe.

To begin the assay, a standard spray bottle was used to spray a mist of water into the air. The glass plate was then swept through the mist to collect a very fine mist of water droplets that covered the plate. One actively mobile larva was then taken from the damp kimwipe and placed in the middle of the misted glass plate. Video recording was started as soon as the larva began to crawl. At 5 seconds the barrier filter was removed to allow the 480nm blue light to pass through to the larva. After 5 seconds the barrier filter was reinserted to stop the blue light. After a final 5 seconds the video was stopped. This gave a video that was recorded at 60 frames/sec for a total of 15 seconds with 5 seconds no light, 5 seconds blue light, and 5 seconds no light at the end. This procedure was repeated for approximately 30 larvae. The video was analyzed as described below.

Video Processing and Analysis

MOV formatted videos were converted to AVI, which is compatible for import into Image J. Image J was then used to process the videos and convert into numerical data for both change in larval length and larval movement.

The first Image J processing function used was to convert the video to grayscale (Fig. 13A). The first frame that the plate comes into contact with the cold surface was then determined visually and set as the first frame used in data analysis. The threshold function was used to create the clearest possible larval silhouettes in all frames. Once the silhouettes are created, the video was converted to binary form, which showed a black silhouette of the larva against a white background. Once in binary form, the skeletonize function was used to transform the larva into linear form Each larva was selected separately and particles

were analyzed for length data (length corresponds to the cringing behavior). The length was collected via the area function under particle analysis.

Length data (read as area in Image J) was then imported into excel for analysis (Fig. 13B). The desired form of this data was percent "cringe". This is defined as the percent length change compared to the maximum length of the larva. The equation used to calculate this is the following: (MAX length – length for each frame)/MAX length. The average maximum % cringe for each larva was taken during the first 1.5s after contact with the cold surface for the cold behavioral assay or between 5 and 6.5 seconds for the optogenetic assay (See Results; Fig. 13C). The average of approximately100 larva per sample for the cold behavioral assay and ~30 larvae for the optogenetic assay were calculated as the average maximum percent cringe.

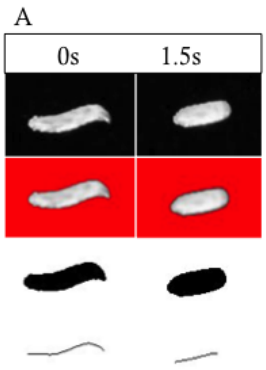

B

Time (s)	Length (# of pixels)	% Cringe
0.0	80	0
0.1	78	2.5
0.2	77	3.75
0.3	77	3.75
0.4	68	15
0.5	59	26.25
0.6	62	22.5
0.7	55	31.25
0.8	59	26.25
0.9	58	27.5
1.0	54	32.5
1.1	51	36.25
1.2	49	38.75
1.3	48	40
1.4	48	40
1.5	47	41.25

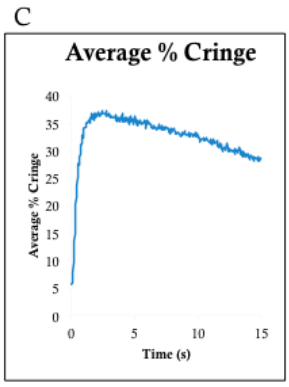

Figure 13. Image processing and calculation of percent cringe. In panel A the first row shows an image of the raw video. Next the threshold function is used to separate the pixels based on brightness in the second row. The pixels are then converted to binary form (third row), which separates them into black and white based on the previously determined threshold. Finally the larvae are converted to linear form via the skeletonize function (fourth row). The larvae in this figure are wild-type Oregon R seen at 0s (before cringing) on the left and 1.5s (during cringing) on the right. Panel B shows the percent cringe data after calculation from pixel data. Finally panel C shows a representation of a full length (15s) larvae video plotted as average percent cringe over time.

Statistical Analysis

Significance of cringe results in the cold plate behavioral assays and optogenetics assays were analyzed by a t-test using a two-sample equal variance (homoscedastic) test (form of t-test). The statistical tests compared experimental genotypes to control genotypes.

RESULTS

Cold Behavioral Assay

The cold behavioral assay was used to determine if any of the three *ppk* genes, *ppk12, ppk23,* and *ppk25,* were necessary for noxious cold detection. A total of nine experimental groups were tested with the cold behavioral assay (Fig. 14). These groups included a known positive control for cringe behavior inhibition, UAS TNTE crossed to the GAL4 driver 19-12 tdGFP, five UAS RNAi constructs crossed to 19-12 tdGFP including UAS *ppk12A*, UAS *ppk23*, and UAS *ppk25A-C,* and three mutant alleles including *ppk12* mutant, and *ppk23* mutants A and B. There were also seven control groups including the negative control wild-type Oregon R which was used as the baseline for a full cringe response, and Oregon R crossed to each of the five UAS RNAi lines and the UAS TNTE line.

The cringe response over time for the experimental and control larvae is shown (Fig. 14). The wild-type (Oregon R) cringe response peaks within 1.5 seconds from beginning of contact with the cold surface (blue traces, Fig. 14). The average maximum percent cringe for wild type larvae was 41.7 % (Figs. 14 and 15; Table 4). In contrast, driving expression of the UAS TNTE delayed the maximum cringe by more than a second, with the greatest percent occurring between 2.5 and 3 seconds (Fig. 14; Table 4). In addition, the maximum average percent cringe for the TNTE control is only 28.4%. This verifies that third instar larvae have a stereotypical response to noxious cold and this response can be negatively affected by expressing the tetanus toxin in CIII da neurons. The data from this positive control revealed two important points. The first is that the peak cringe appears to be delayed compared to Oregon R. The second is that the peak cringe is lower during the course of the assay. Therefore in order to quantify the results, the average maximum percent cringe within the first 1.5 seconds for the larvae in the control groups were compared to that for the experimental groups. In this way it was possible to capitalize on both delayed response and smaller cringe in order to give statistical significance between the experimental and control groups.

There was a significant alteration of the cringe response when *ppk* RNAi was expressed in third instar larvae (Fig. 14; Table 4). The control crosses for all five *ppk* RNAi constructs mimicked the wild-type crosses. Maximum percent cringe for these controls ranged from 38.7-43.5% as compared to 41.7% for Oregon R (Table 4). This suggests the undriven UAS RNAi transgenes do not change the maximum percent cringe. Further, the timing and overall cringe response resembles that of the Oregon R control (Fig.

14, compare blue trace to red traces). These controls contrast the experimental CIII driven experimental *ppk* RNAi lines. All five GAL4 driven *ppk* RNAi constructs exhibited a delay in reaching their maximum percent cringe (Fig. 14). The delay in reaching their maximum as compared to Oregon R was approximately 1.5 seconds for UAS *ppk12A*, UAS *ppk23*, UAS *ppk25A* and UAS *ppk25C* and approximately 3 seconds for UAS *ppk25B* (Fig. 14). When comparing the percent cringe at 1.5 seconds of the assay, all of the experimental larvae showed a lower amount of cringing, ranging from 31.7-36.0% compared to 41.7% for Oregon R (Fig. 15; Table 4). While this reduction in cringing is not as great as for the TNTE experimental (28.7%), statistical analysis using a Type 2, 2 tailed T-Test showed the values were significantly different ($p < 0.001$; Fig 15). Even when maximum percent cringe was achieved by each experimental set, it was lower than the Oregon R control (Fig. 14). Three mutant alleles, *ppk12* and two *ppk23* mutant alleles, exhibited comparable results with their RNAi experimental counterparts (Figs. 14 and 16; Table 4).

Table 4: Maximum Percent Cringe at 1.5 Seconds in Behavioral Assay

Larvae Type	**Experimental[1] (n)**	**Control[2] (n)**
Oregon R	41.7% (90)	N/A[3]
TNTE	28.7% (107)	38.7% (109)
ppk12, RNAi line A	35.8% (108)	43.5% (95)
ppk12, mutant	36.3% (100)	N/A
ppk23, RNAi	36.0% (117)	41.8% (102)
ppk23, mutant allele A	35.1% (103)	N/A
ppk23, mutant allele B	31.3% (61)	N/A
ppk25, RNAi line A	35.7% (87)	40.2% (94)
ppk25, RNAi line B	31.7% (108)	41.6% (111)
ppk25, RNAi line C	34.2% (114)	41.2% (104)

1: Experimental larvae were the indicated UAS RNAi line crossed the CIII da neuron Gal4 driver.
2: Control larvae were the indicated UAS RNAi line outcrossed to Oregon R.
3: Not Applicable.

Blue = wild type OR (control)
Red = wild type OR X UAS RNAi (control)
Green = 19-12 tdGFP X UAS RNAi and mutants (experimental)

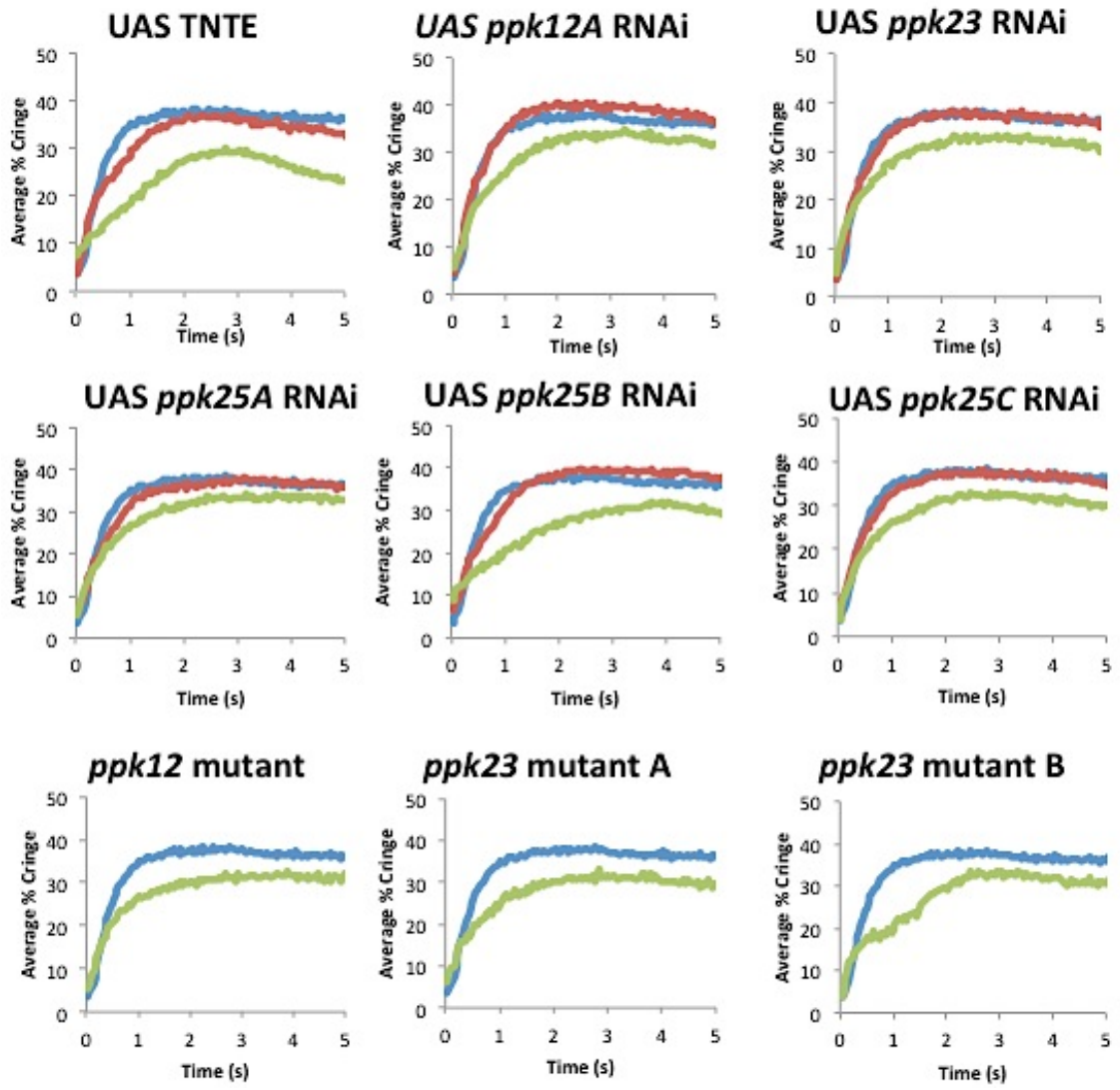

Figure 14. Cold behavioral assay results expressed as average percent cringe over time. 61-117 larvae were assayed for each trial. 5°C was used as the stimulus. *ppk25A-C* refer to three separate *ppk25* RNAi constructs while *ppk23* mutant A and B refer to different *ppk23* mutants. Exact genotypes and stock numbers can be found in Tables 1 and 2. Blue trace represent wild type Oregon R, red traces represent Oregon R X corresponding UAS RNAi controls, and green traces represent either 19-12 tdGFP X corresponding UAS RNAi or mutant experimental larvae. Data is shown for the first 5 seconds after contact with the 5°C cold surface.

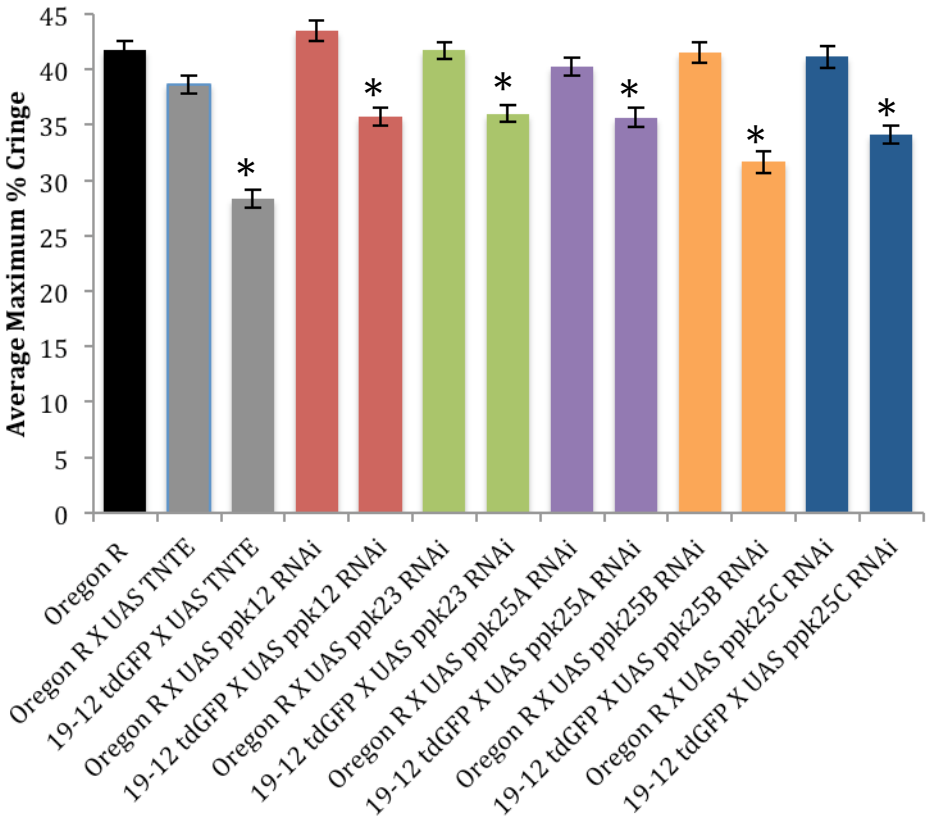

Figure 15. Cold behavioral assay RNAi results. 61-117 larvae were assayed for each trial. The number of larvae tested for each genotype is shown in Table 4. Type 2, 2 tailed t-tests were used to determine significance with p-values less than .001 accepted as significant and indicated by *. T-tests were performed comparing experimental to WT and – controls (UAS RNAi constructs not crossed to GAL4 19-12 driver). Error bars represent the SEM. *ppk25A-C* refer to three separate *ppk25* constructs. Exact genotypes and stock numbers can be found in Tables 1 and 2.

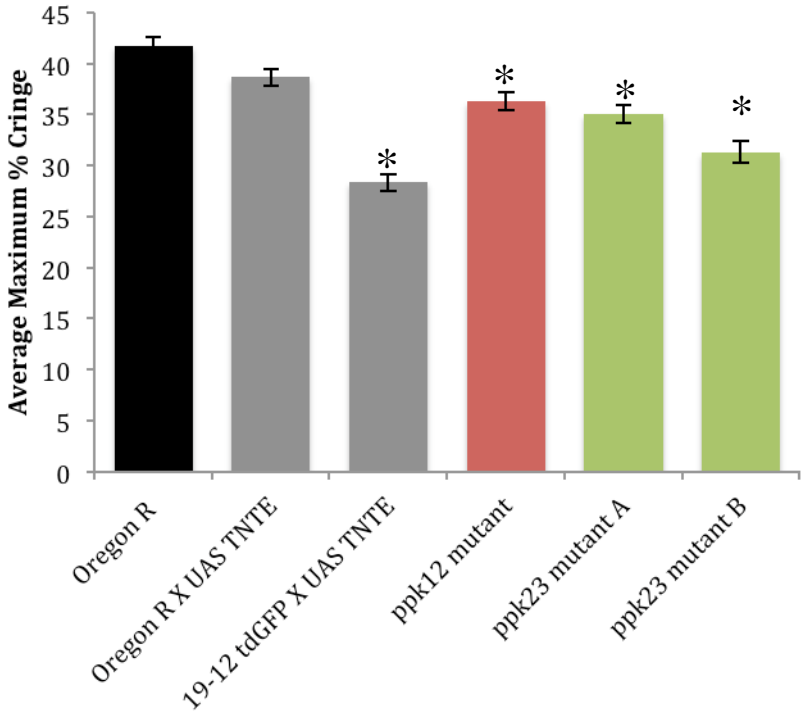

Figure 16. Cold Behavioral Assay Mutant Results. 61-117 larvae were assayed for each trial. 5°C was used as the stimulus. *ppk23* mutant A and B refer to different *ppk23* mutants. Type 2, 2 tailed t-tests were used to determine significance with p-values less than .001 accepted as significant and indicated by *. T-tests were performed comparing experimental to WT. Error bars represent the SEM. Exact genotypes and stock numbers can be found in Table 1.

Optogenetic Assay

The cold behavioral assays suggested *ppk12, ppk23,* and *ppk25* function in detection of noxious cold. The optogenetic assay helped determine whether these three *ppk* genes function in noxious cold transduction or propagation. A total of seven experimental groups were performed for the cold behavioral assay. These groups included the known positive control for cringe behavior inhibition, UAS TNTE crossed to the GAL4 driver 19-12 ChETA, and six UAS RNAi constructs crossed to 19-12 ChETA including UAS *ppk12A*, UAS *ppk12B,* UAS *ppk23*, and UAS *ppk25A-C.* The experimental larvae were fed the ATR cofactor while the control larvae were the same genotype but were not fed ATR. For comparison three cringe control groups were tested. Wildtype larvae expressing 19-12 ChETA fed ATR served as the control for a full cringe response upon blue light stimulation (Fig. 17, blue traces);, 19-12 ChETA larvae not fed ATR and the UAS TNTE X 19-12 ChETA larvae also served as controls (Fig. 17, red traces).

There was a significant alteration of the cringe response only when *ppk25* RNAi was expressed in third instar larvae (Fig. 18; Table 5). However, visually in figure 17 it can be seen that cringe still appears to be inhibited in all UAS ppk RNAi larvae. Maximum percent cringe for the positive cringe inhibition controls (19-12 ChETA larvae not fed ATR and the UAS TNTE X 19-12 ChETA larvae with and without ATR) ranged from 22.7-27.1% as compared to 50.6% for 19-12 ChETA larvae fed ATR (Table 5). This shows that both ATR is necessary for a full cringe response, and that TNTE is equally powerful as absence of ATR in inhibiting this response. These controls contrast the experimental CIII driven experimental *ppk25* RNAi lines. When comparing the maximum percent cringe from 5-6.5 seconds of the assay, *ppk12* and *ppk23* RNAi larvae were not significantly inhibited in their cringe response ranging from 39.7-48.1%. Only the experimental larvae for *ppk25* RNAi showed a significantly lower amount of cringing, ranging from 29.3 - 43.1% compared to 50.6% for 19-12 ChETA with ATR (Fig. 18; Table 5). While this reduction in cringing is not as great as for the TNTE experimental (22.7%), statistical analysis using a Type 2, 2 tailed T-Test showed the values were significantly different ($p < 0.001$; Fig 18). Even when maximum percent cringe was achieved by each experimental set, it was lower than the 19-12 ChETA with ATR control (Fig. 17).

Table 5: Maximum Percent Cringe from 5-6.5 Seconds in Optogenetic Assay

Larvae Type	**Experimental[1] (with ATR) (n)**	**Control[2] (without ATR) (n)**
19-12 ChETA	50.6% (50)	27.1% (10)
TNTE	22.7%(15)	25.8% (16)
ppk12, RNAi line A	44.3% (19)	N/A[3]
ppk12, RNAi line A	39.7%(5)	N/A
ppk23, RNAi	48.1% (55)	N/A
ppk25, RNAi line A	43.1% (23)	N/A
ppk25, RNAi line B	35.9% (41)	N/A
ppk25, RNAi line C	29.3% (29)	N/A

1: Experimental larvae were the indicated UAS RNAi line crossed to the CIII da neuron Gal4 driver 19-12 ChETA with ATR.
2: Control larvae were the indicated UAS RNAi line crossed to 19-12 ChETA without ATR.
3: Not Applicable.

The cringe response over time for the experimental and control larvae is shown (Fig. 17). Again, the blue light stimulus was only active between the five and ten second time points. The 19-12 ChETA with ATR cringe response peaks in less than a second from beginning of blue light activation (blue traces, Fig. 17). The average maximum percent cringe for 19-12 ChETA with ATR larvae was 50.6 percent (Fig. 18).

In contrast, the maximum average percent cringe for the 19-12 ChETA driven UAS TNTE with ATR control is only 22.7 percent. Both the 19-12 CheTA and 19-12 ChETA driven UAS TNTE had significantly inhibited cringe responses without ATR (27.1 and 25.8 percent respectively). This verifies that third instar larvae have a stereotypical response to blue light activation that requires the presence of ATR and mimics the response to cold. This response can be negatively affected by expressing the tetanus toxin in CIII da neurons. In this assay no delay was seen for any of the positive controls.

The data from these positive controls gave three important points. The first is that ATR is absolutely necessary for the cringe response to blue light. The second is that the peak cringe is lower during the course of the assay. And the third is that there appears to be no delay in the cringe response. Therefore in order to quantify the results, the exact same procedure was used in that the average maximum percent cringe within the first 1.5 seconds after blue light activation for the larvae in the control groups were compared to that for the experimental groups.

For comparison, the average maximum percent cringe for the 19-12 ChETA with ATR was 50.6 percent. The average maximum percent cringe for 19-12 ChETA X UAS ppk12A with ATR was 44.3 percent, for 19-12 ChETA X UAS ppk12B with ATR was 39.7 percent, for the 19-12 ChETA X UAS ppk 23 with ATR was 48.1 percent, for 19-12 ChETA X UAS ppk 25A with ATR was 43.1 percent, for the 19-12 ChETA X UAS ppk25B with ATR was 35.9 percent, and for 19-12 ChETA X UAS ppk25C with ATR was 29.3 percent. All crosses were performed without ATR as another control (data not shown).

Blue = 19-12 ChETA w/ ATR (control)
Red = 19-12 ChETA w/o ATR (control)
Green = 19-12 ChETA X UAS RNAi or UAS TNTE (experimental)

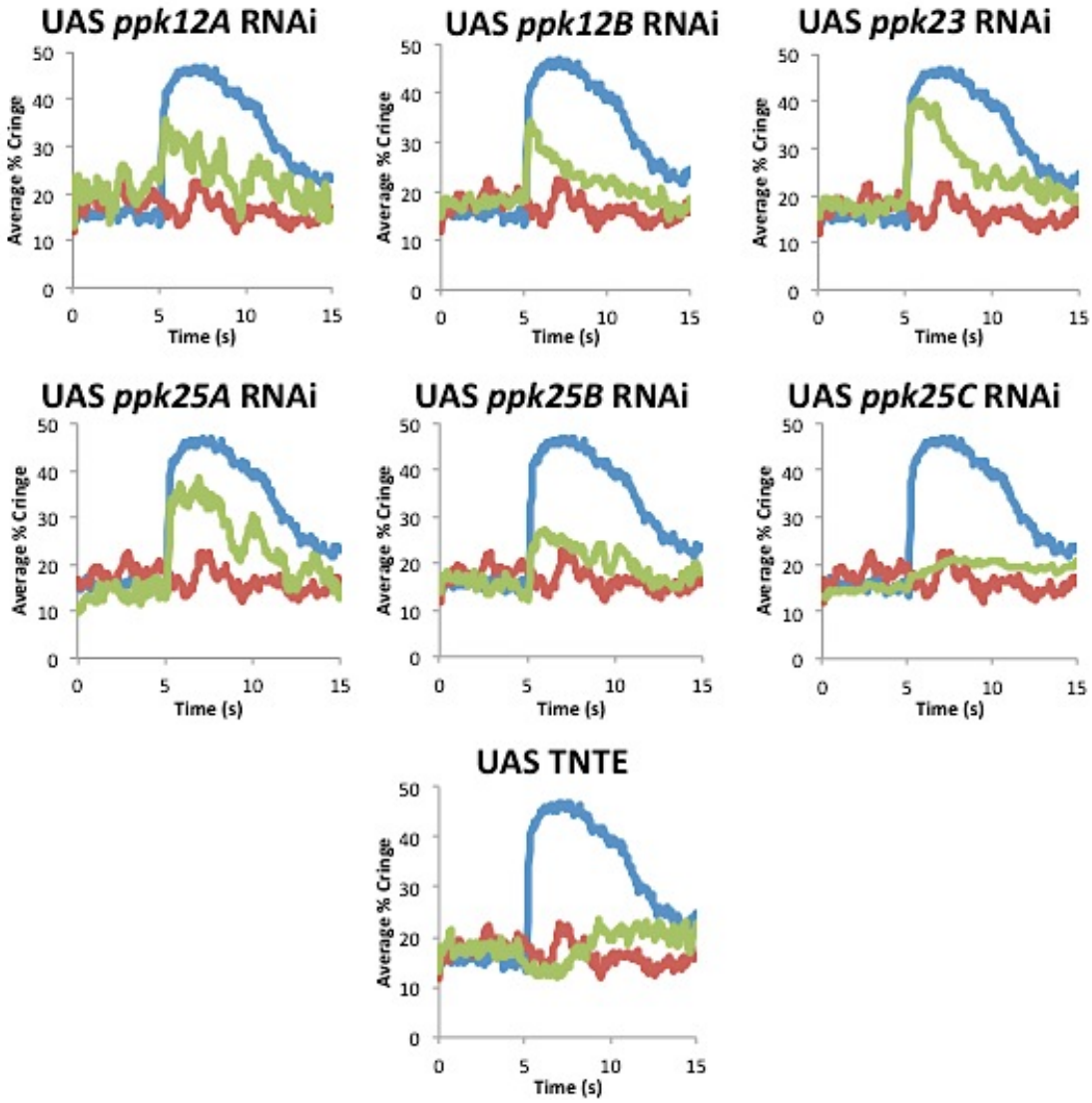

Figure 17. Optogenetic assay results expressed as average percent cringe over time. Approximately 5-50 larvae were assayed for each trial. 5 seconds of blue light was used as the stimulus. The assay began with 5 seconds of dark, followed by 5 seconds of blue light, followed again by 5 seconds of dark. Exact genotypes and stock numbers can be found in table 1. Blue traces represent 19-12 ChETA w/ ATR, red traces represent 19-12 ChETA without ATR control, and green traces represent 19-12 ChETA X corresponding UAS RNAi or UAS TNTE w/ ATR experimental larvae. The beginning of the stimulus was directly at the 5 second time point and lasts until the 10 second time point.

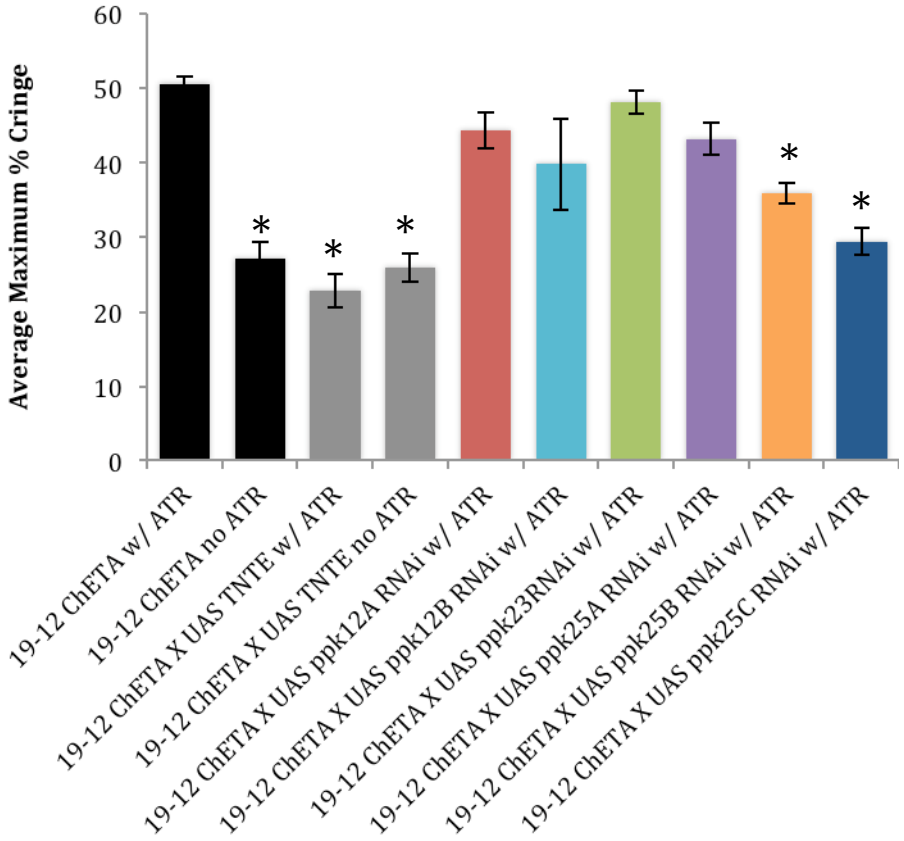

Figure 18. Optogenetic assay average maximum percent cringe results. 5-50 larvae were assayed for each trial. 5 seconds of blue light was used as the stimulus. Type 2, 2 tailed t-tests were used to determine significance with p-values less than .001 accepted as significant and indicated by *. T-tests were performed comparing to ChETA with ATR. Error bars represent the SEM. Exact genotypes and stock numbers can be found in Tables 1 and 3.

DISCUSSION

Statement of Hypothesis and Predicted Experimental Results

The original hypothesis predicted at least one of the three members of the DEG/ENaC *pickpocket* family (*ppk12, ppk23,* and *ppk25*) function in class III da neurons to mediate the larva's nociceptive cold behavioral response. Further, that each might affect either the transduction of the cold sensing or subsequent propagation of that sensing within the class III da neurons. These hypotheses were examined in larvae expressing RNAi transgenes or bearing loss-of-function mutant alleles as compared to appropriate controls. Any statistically significant inhibition in the cringing response from RNAi expression driven in CIII da neurons was interpreted as the gene product possibly playing a functional role in cold nociception. Separately created RNAi lines and mutants were used to validate the observations. Finally the genes were tested using an optogenetic assay to better clarify the channel function in the cold behavioral response (Figs. 4 and 11). If there was a significant inhibition of the cringe response, it was concluded that the gene was likely involved in the propagation of the action potential generated by the noxious cold stimulus given that optogenetic activation alone is sufficient to elicit the cringe response in the absence of the stimulus. However, if the cringe response was wild-type, it was concluded that the gene was likely involved in the transduction step of the noxious stimulus. Preliminary data from the Cox lab has demonstrated, for example, that the TRP channels*, nompC, Pkd2*, and *trpm* function in the transduction step consistent with members of the TRP family, whereas the *para* gene, is involved in the propagation phase of the response.

Cold Behavioral Assay

The hypothesis for the cold assay was that *ppk12, ppk23,* and *ppk25* could function in cold detection. The prediction for the cold behavioral assay was that all 5 RNAi constructs (*ppk12, ppk23,* and *ppk25A-C)* and 3 mutants (*ppk12* mutant*, ppk23* mutant A, and *ppk23* mutant B) would inhibit the cringe response to noxious cold. More specifically this data would be visible as significant decreases in the average maximum percent cringe compared to the wild type Oregon R control and to the specific UAS X Oregon R controls. The results of the cold behavioral assay did exhibit significant decreases in the average maximum percent cringe (p values $\leq .001$) during the first 1.5 seconds after exposure to noxious cold for all experimental groups. The 19-12 tdGFP X UAS TNTE group had the most significant inhibition with a maximum percent cringe of only 28.4 percent compared to 41.7 percent in Oregon R, which was at least

2.9 percent lower than any other RNAi construct or mutant. This means that knocking down the individual *ppk* subunits one at a time was not sufficient to completely inhibit the response to cold. This may therefore indicate that knocking down multiple *ppk* subunits could create a stronger effect. It is thought that *ppk23* and *ppk25* form a heterotrimer with *ppk29* involved in pheromone detection, so it may very well be possible that *ppk12* could take the place of *ppk29* to form a cold sensitive channel (Vijayan *et al.* 2012). Other combinations of PPK proteins could be responsible and additional experiments are required to test this possibility. The results of the cold behavioral assay therefore confirmed the hypothesis and indicated that *ppk12, ppk23,* and *ppk25* are all involved in noxious cold detection in some way. Therefore, it was reasonable to test all three of the *ppk* genes in the optogenetic assay.

Optogenetic Assay

The hypothesis for the optogenetic assay predicts that if *ppk12, ppk23,* and/or *ppk25* contribute to the noxious cold response as indicated by the cold behavioral assay, then they would function in either the transduction or propagation phase of the response. Only the *ppk25A-C B* and *C* RNAi constructs significantly inhibited the blue light activated cringe response (35.943.1, and, 35.9, and 29.3 average maximum percent cringes respectively; Fig. 18) compared to 50.6 average maximum percent cringe in the 19-12 ChETA with ATR. Therefore, *ppk25* is likely to be involved in the propagation phase of cold detection within the CIII da neuron.

DEG/ENaC subunits are known to function in both propagation and transduction of mechanical stimuli, it possible that either *ppk12* and *ppk23* could function in either transduction or propagation. (Zhong 2011, Raouf *et al.* 2012). *ppk12* and *ppk23* did not significantly inhibit the cringe response (Fig. 18). This suggests they affect the transduction phase. However, since only two RNAi constructs were tested for *ppk12* and only one RNAi construct was tested for *ppk23,* the possibility of these genes being involved in propagation cannot yet be ruled out. Examining their impact over time in the optogenetic assay (Fig. 17), it does appear there is an inhibition of the cringe response even though it is not statistically significant. The statistical insignificance may be due to mutual dependence of the subunits to form a heteromeric channel. In other systems, mutant alleles for these genes would presumably result in a knock out of gene function as

opposed to a knock down by RNAi expression. Future work with mutant alleles for each of these genes in the optogenetic assay may clarify the function of these genes in noxious cold detection.

Overall, I think it most likely that all three *pickpocket* genes are involved in the propagation phase of noxious cold detection. My reasoning is that our assay was developed to avoid false positive results which made it less sensitive to small effects, and based on the graphical data in Figure 17, it seems entirely possible that all genes tested were involved in propagation.

An important observation worth mentioning was the high variation between individual larvae in the optogenetic assay. More specifically, it was noted during video recording that some larva cringed as if they did not have RNAi while others appeared to be inhibited. Typically, there should not be phenotypic differences between genetically identical larvae. This variability was difficult to quantify and cannot be seen in the calculated data, but was most pronounced in *ppk23* RNAi constructs. Due to the specificity of this observation to *ppk23*, an explanation may be due to the location of insertion. It is known that when genes that normally located in euchromatin become inserted into heterochromatic regions, this can result in random silencing of the gene. This can in turn cause phenotypic differences between individual larvae, which are of the same genotype and is called position effect variegation (Elgin and Reuter, 2013). It is our hypothesis that although the insertion point of our *ppk23* RNAi construct (KK106873-VDRC) is unknown, that it may have been inserted near a heterochromatic region of the chromosome. The significance of this observation is that random strength of knockdown from the RNAi insertion may cause the data to more closely resemble wild-type, and therefore behavioral changes may be missed.

Future Directions

Future directions for this project include three major sets of experiments. The first is to assay mutant *ppk* lines in the optogenetic assay. This could validated the RNAi results that *ppk25* likely functions during propagation. In addition, mutant analysis could clarify the roles of *ppk12* and *ppk23.* The second set of experiments will include co-expression studies of *ppk12, ppk23,* and *ppk25* to help determine if the effect is stronger when these genes are working in combination. Work by Dan Cox's lab has already given insight to co-expression of these genes, and will be used to determine the course of action for this set of experiments. The hypothesis is these co-expression studies will yield information not only on the function

of these genes, but also how their encoded subunits fit together. The third set of experiments would be a microscopic analysis to determine the localization of *ppk12, ppk23,* and *ppk25* in the CIII neurons. A very similar study was conducted by Gorczyca *et. al* (2014) in which they created rabbit anti *ppk1* and *ppk26* antibodies with mCherry and EGFP fluorescent tags. This may give more insight into the functional roles of these genes. The prediction is that those involved in transduction will be localized to the extremities of the dendrites where they integrate the epidermis, while those involved in propagation will be localized along the axon of the neuron. It may also help to show visually if the subunits are co-localized indicating that they form heteromers.

Significance

This study has identified three genes, *ppk12, ppk23,* and *ppk25,* that are likely to be involved in noxious cold detection, and it is likely that at least one of them (*ppk25)* functions in propagation. Only TRPM8 and TRPA1 are known to be involved in noxious cold detection in mammals (Feketa *et al.* 1997). Therefore it is possible that DEG/ENaC genes may also be involved in noxious cold detection in mammals. This may lead to new potential targets for the treatment of pain.

Of a broader significance, this work has helped to fill the gap in understanding the mechanisms of all pain evoking stimuli. Similarities and differences between genes involved in each stimuli may help to both decipher what is common to all types of nociception as well as what is specific to each stimulus.

REFERENCES

Adams CM, Anderson MG, Motto DG, Price MP, Johnson WA, Welsh MJ. 1998. Ripped pocket and pickpocket, novel Drosophila DEG/ENaC subunits expressed in early development.. J Cell Biol. 140143.

Akerboom J, Chen T, Wardill TJ, Tian L, Marvin JS, Mutlu S, Calderón NC, Esposti F, Borghuis BG, Sun XR, et al. 2012. Optimization of a GCaMP calcium indicator for neural activity imaging. J Neurosci. 32:13819-40.

Aldrich BT, Kasuya J, Faron M, Ishimoto H, Kitamoto T. 2010. The amnesiac gene is involved in the regulation of thermal nociception in Drosophila melanogaster. J Neurogenet. 24:33-41.

Bachmann A, Knust E. 2008. The use of P-element transposons to generate transgenic flies. Methods Mol Biol. 420:61-77.

Bamberg, E. 2014. Professor Biography Website for Prof. Dr. Ernst Bamberg. Max-Planck-Institut für Biophysik, Frankfurt. http://www.biophys.mpg.de/en/bamberg.html

Bianchi L, Driscoll M. Minireview: Protons at the gate. DEG/ENaC ion channels help us feel and remember. Neuron. 34:337-40.

Caro LN, Moreau CJ, Estrada-Mondragon A, Ernst OP, Vivaudou, M. 2012. Engineering of an artificial light-modulated potassium channel. Plos One 7:1-9.

Clapham, DE, .Runnels LW, Strübing, C. 2001. The TRP ion channel family. Nat Rev Neurosci. 2:387-96.

Coordination and Response. c2012. XtremePapers [accessed 2015 April 10]. https://www.xtremepapers.com/revision/gcse/biology/co-ordination_and_response.php

Cosens DJ and Manning A. 1969. Abnormal electroretinogram from a Drosophila mutant. Nature. 224:285-7.

Duffy JB. 2002. GAL4 system in Drosophila: A fly geneticist's swiss army knife. Genesis. 34:1-15.

Elgin SCR, Reuter G. 2013. Position-effect variegation, heterochromatin formation, and gene silencing in Drosophila. Cold Spring Harb Perspect Biol. 5:a017780.

Feketa VV, Zhang Y, Cao Z, Balasubramanian A, Flores CM, Player MR, Marrelli SP. 2014. Transient receptor potential melastatin 8 channel inhibition potentiates the hypothermic response to transient receptor potential vanilloid 1 activation in the conscious mouse. Crit Care Med. 42:e355-63.

Gallio M, Ofstad TA, Macpherson LJ, Wang JW, Zuker CS. 2011. The coding of temperature in the Drosophila brain. Cell 144:614-24.

Gautam M, Benson CJ. 2013. Acid-sensing ion channels (ASICs) in mouse skeletal muscle afferents are heteromers composed of ASIC1a, ASIC2, and ASIC3 subunits. FASEB J. 27:793.

Gorczyca DA, Younger S, Meltzer S, Kim SE, Cheng L, Song W, Lee HY, Jan LY, Jan YN. 2014. Article: Identification of Ppk26, a DEG/ENaC channel functioning with Ppk1 in a mutually dependent manner to guide locomotion behavior in Drosophila. Cell Rep. 9:1446-58.

Grueber WB, Jan LY, Jan YN. 2002. Tiling of the Drosophila epidermis by multidendritic sensory neurons. Development. 129:2867-78.

Honjo K, Hwang RY, Tracey,WD,,Jr. 2012. Optogenetic manipulation of neural circuits and behavior in Drosophila larvae. Nat Protoc. 7:1470-8.

Husson SJ, Gottschalk A, Leifer AM. 2013. Optogenetic manipulation of neural activity in C. elegans: From synapse to circuits and behaviour. Biol Cell. 105:235-50.

Im SH, Galko MJ. 2012. Pokes, sunburn, and hot sauce: Drosophila as an emerging model for the biology of nociception. Dev Dyn. 241:16-26.

Iyer EPR, Iyer SC, Sullivan L, Wang D, Meduri R, Graybeal LL, Cox DN. 2013. Functional genomic analyses of two morphologically distinct classes of drosophila sensory neurons: Post-mitotic roles of transcription factors in dendritic patterning. Plos One. 8:1-16.

Iyer SC, Ramachandran Iyer EP, Meduri R, Rubaharan M, Kuntimaddi A, Karamsetty M, Cox DN. 2013. Cut, via CrebA, transcriptionally regulates the COPII secretory pathway to direct dendrite development in Drosophila. J Cell Sci. 126:4732-45.

Jegla TJ, Zmasek CM, Batalov S, Nayak SK. 2009. Evolution of the human ion channel set. Comb Chem High Throughput Screen. 12:2-23.

Jeong, S., Lee, S. H., Kim, Y. O., & Yoon, M. H. 2013. Antinociceptive Effects of Amiloride and Benzamil in Neuropathic Pain Model Rats. J Korean Med Sci. 28:1238–1243.

Jian-Quan Ni, Markstein M, Binari R, Pfeiffer B, Lu-Ping Liu, Villalta C, Booker M, Perkins L, Perrimon N. 2008. Vector and parameters for targeted transgenic RNA interference in Drosophila melanogaster. Nat Methods. 5:49-51.

Khuong TM, Neely GG. 2013. Conserved systems and functional genomic assessment of nociception. J FEBS J. 280:5298-306.

Kim SE, Coste B, Chadha A, Cook B, Patapoutian A. 2012. The role of Drosophila Piezo in mechanical nociception. Nature. 483:209-12.

Liu L, Johnson WA, Welsh MJ. 2003. Drosophila DEG/ENaC pickpocket genes are expressed in the tracheal system, where they may be involved in liquid clearance. Proc Natl Acad Sci USA. 100:2128-33.

Loeser JD, Treede R. 2008. The Kyoto protocol of IASP basic pain terminology. Pain 137:473-7.

Lu B, LaMora A, Sun Y, Welsh MJ, Ben-Shahar Y. 2012. ppk23-Dependent chemosensory functions contribute to courtship behavior in drosophila melanogaster. PLoS Genet. 8:1-13.

Milinkeviciute G, Gentile C, Neely GG. 2012. Drosophila as a tool for studying the conserved genetics of pain. Clin Genet. 82:359-66.

Minke B. 2010. The history of the Drosophila TRP channel: The birth of a new channel superfamily. J Neurogenet. 24:216-33.

Montell C. 2005. Drosophila TRP channels. Pflugers Arch. 451:19-28.

Orgogozo V and Grueber WB. 2005. FlyPNS, a database of the Drosophila embryonic and larval peripheral nervous system. BMC Dev Biol. 5:4.

Pikielny CW. 2012. Sexy DEG/ENaC channels involved in gustatory detection of fruit fly pheromones. Sci Signal. 5:pe48.

Prüßing K, Voigt A, Schulz J. 2013. Drosophila melanogaster as a model organism for alzheimer's disease. Mol Neurodegener. 8:35.

Raouf R, Rugiero F, Kiesewetter H, Hatch R, Hummler E, Nassar MA, Wang F, Wood JN. 2012. Sodium channels and mammalian sensory mechanotransduction. Mol Pain. 8:21.

Rosenzweig M, Kang K, Garrity PA. 2008. Distinct TRP channels are required for warm and cool avoidance in drosophila melanogaster. Proc Natl Acad Sci USA. 105:14668-73.

Salat K, Moniczewski A, Librowski T. 2013. Transient receptor potential channels - emerging novel drug targets for the treatment of pain. Curr Med Chem. 20:1409-36.

Singh S, Ganguli I. 2013. RNA interference technology: Implications and applications. Agricultural Reviews 34:62-70.

Slater D, Kunnathil S, McBride J, Koppala R. 2010. Pharmacology of nonsteroidal antiinflammatory drugs and opioids. Semin Intervent Radiol. 27:400-11.

Sulkowski MJ, Kurosawa MS, Cox DN. 2011. Growing pains: Development of the larval nocifensive response in Drosophila. Biol Bull. 221:300-6.

Sullivan, S., Iyet, S.C., Armengol, K., Iyer, E.P.R., and Cox, D.N. 2013. Investigating the cellular basis of cold nociception in Drosophila larvae. 54th Annual *Drosophila* Research Conference, Washington, D.C.

Sweeney ST, Broadie K, Keane J, Niemann H, O'Kane ,CJ. 1995. Targeted expression of tetanus toxin light chain in Drosophila specifically eliminates synaptic transmission and causes behavioral defects. Neuron. 14:341-51.

Tracey Jr. WD, Wilson RI, Laurent G, Benzer S. 2003. painless, a Drosophila gene essential for nociception. Cell. 113:261-73.

Umezaki Y, Yasuyama K, Nakagoshi H, Tomioka K. 2011. Blocking synaptic transmission with tetanus toxin light chain reveals modes of neurotransmission in the PDF-positive circadian clock neurons of Drosophila melanogaster. J Insect Physiol. 57:1290-9.

Vergara C, Latorre R, Marrion NV, Adelman JP. 1998. Calcium-activated potassium channels. Curr Opin Neurobiol. 8:321-9.

Vijayan V, Thistle R, Liu, Tong, Starostina E, Pikielny, CW. 2014. Drosophila pheromone-sensing neurons expressing the ppk25 ion channel subunit stimulate male courtship and female receptivity. PLoS Genet. 10:e1004238.

Wong GY, Gavva NR. 2009. Therapeutic potential of vanilloid receptor TRPV1 agonists and antagonists as analgesics: Recent advances and setbacks. Brain Res Rev. 60:267-77.

Wong J, Abilez OJ, Kuhl E. 2012. Computational optogenetics: A novel continuum framework for the photoelectrochemistry of living systems. J Mech Phys Solids. 60:1158-78.

Zelle KM, Lu B, Pyfrom SC, Ben-Shahar Y. 2013. The genetic architecture of degenerin/epithelial sodium channels in Drosophila. G3 (Bethesda) 3:441-50.

Zha X, et al. 2009. Oxidant regulated inter-subunit disulfide bond formation between ASICIa subunits. Proc Natl Acad Sci USA. (9):3573-8.

Zhong L, Hwang RY, Tracey WD. 2010. Pickpocket is a DEG/ENaC protein required for mechanical nociception in Drosophila larvae. Curr Biol. 20:429-34.

Zhong L. 2011. Neuronal and molecular basis of nociception and thermosensation in Drosophila melanogaster [dissertation]. [Durham (NC)]: Duke University.

APPENDIXES

Table S1. Raw Data for Cold Behavioral Assay

Genotype	**n**	**Average**	**Standard Deviation**	**SEM**	**p-value from Oregon R**	**p-value from UASXOR**
Oregon R	90	41.74	8.10	0.85		
Oregon R X UAS TNTE	109	38.68	8.68	0.83	1.14E-02	
19-12 tdGFP X UAS TNTE	107	28.40	8.42	0.81	5.12E-23	3.81E-16
Oregon R X UAS *ppk12A* RNAi	95	43.53	9.21	0.95	1.65E-01	
19-12 tdGFP X UAS *ppk12A* RNAi	108	35.75	8.36	0.80	8.00E-07	1.75E-09
Oregon R X UAS *ppk23* RNAi	102	41.75	7.65	0.76	9.98E-01	
19-12 tdGFP X UAS *ppk23* RNAi	117	36.04	8.08	0.75	1.09E-06	2.33E-07
Oregon R X UAS *ppk25A* RNAi	94	40.24	8.76	0.90	2.29E-01	
19-12 tdGFP X UAS *ppk25A* RNAi	87	35.71	9.14	0.98	6.41E-06	8.09E-04
Oregon R X UAS *ppk25B* RNAi	111	41.55	8.68	0.82	8.61E-01	
19-12 tdGFP X UAS *ppk25B* RNAi	108	31.68	8.91	0.86	2.35E-14	9.26E-15
Oregon R X UAS *ppk25C* RNAi	104	41.16	10.07	0.99	6.62E-01	
19-12 tdGFP X UAS *ppk25C* RNAi	114	34.16	9.06	0.85	2.83E-09	1.69E-07
ppk12 Mutant	100	36.29	8.81	0.88	1.65E-05	
ppk23 Mutant A	103	35.08	8.78	0.87	1.56E-07	
ppk23 Mutant B	61	31.30	8.43	1.08	2.34E-12	

Table S2. Raw Data for Optogenetic Assay

Genotype	**n**	**Average**	**Standard Deviation**	**SEM**	**p-value from 19-12 ChETA w/ ATR**
19-12 ChETA w/ ATR	50	50.60	6.18	0.87	
19-12 ChETA no ATR	10	27.07	7.04	2.23	2.05E-15
19-12 ChETA X UAS TNTE w/ ATR	15	22.72	8.83	2.28	1.04E-20
19-12 ChETA X UAS TNTE no ATR	16	25.78	7.57	1.89	5.75E-20
19-12 ChETA X UAS *ppk12A* RNAi w/ ATR	19	44.31	10.38	2.38	2.88E-03
19-12 ChETA X UAS *ppk12B* RNAi w/ ATR	5	39.73	13.57	6.07	1.72E-03
19-12 ChETA X UAS *ppk23* RNAi w/ ATR	55	48.08	11.24	1.52	1.64E-01
19-12 ChETA X UAS *ppk25A* RNAi w/ ATR	23	43.13	10.22	2.13	2.41E-04
19-12 ChETA X UAS *ppk25B* RNAi w/ ATR	41	35.87	8.60	1.34	3.73E-15
19-12 ChETA X UAS *ppk25C* RNAi w/ ATR	29	29.33	9.80	1.82	9.10E-19